Scholars' Mine

Masters Theses

Student Theses and Dissertations

Spring 1985

A study of shadow contrast for a grating

Steve Eugene Watkins
Missouri University of Science and Technology, watkins@mst.edu

Follow this and additional works at: https://scholarsmine.mst.edu/masters_theses

Part of the Electrical and Computer Engineering Commons

Department:

Recommended Citation

A STUDY OF SHADOW CONTRAST

FOR A GRATING

BY

STEVE EUGENE WATKINS, 1960-

A THESIS

Presented to the Faculty of the Graduate School of the

UNIVERSITY OF MISSOURI-ROLLA

In Partial Fulfillment of the Requirements for the Degree

MASTER OF SCIENCE IN ELECTRICAL ENGINEERING

1985

T5203
Copy 1
51 pages

Approved by

Jerome Knopp (Advisor) _David Cunningham_

J. H. Pagano

ABSTRACT

A theoretical and experimental investigation of the causes of the reduction of the contrast in the shadow of a grating has been made. The variation of the shadow contrast is shown to be different for the two causes--diffraction and divergence. The conditions which determine the dominant effect are presented. Also, the contrast pattern due to diffraction is shown to have a squared scaling law while the divergence pattern is shown to scale linearly. This understanding of the shadow contrast increases the versatility and usefulness of the shadow moire technique, an optical method for determining the topography of surfaces.

ACKNOWLEDGEMENT

TABLE OF CONTENTS

LIST OF FIGURES

LIST OF SYMBOLS

A = intensity amplitude factor

C = constant

C.R. = contrast ratio = maximum intensity divided by
minimum intensity

D = distance from the grating to the observation
plane

D' = distance from the source to the grating

E = fraction of energy within an angular width

G = product of the incident field and the grating
transmittance function

g = grating transmittance function

h = impulse response

I = intensity

$j = \sqrt{-1}$

$k = 2\pi/\lambda$ = wave number

L = length of impulse response in the observation
plane

L' = length of effective line source

m = general variable

N = scaling factor

n = general integer

p = grating period

R = aperture perimeter-to-area ratio

$r = \sqrt{x^2+y^2+z^2}$

$$\text{rect}(\tau) = \begin{cases} 1 & |\tau| \leq 1/2 \\ \\ 0 & \text{otherwise} \end{cases}$$

U = complex field

x, y, and z = rectangular coordinates

z = distance from the grating to the observation plane

$\mathcal{F}\{\ \}_f$ = one-dimensional Fourier transform in f

$\mathcal{F}\{\ \}_{f_1, f_2}$ = two-dimensional Fourier transform in f_1 and f_2

β and τ = dummy variables

δ = Dirac delta function

λ = wavelength

π = 3.14159

ϕ = angular half-width

ϕ_d = first order diffraction angle

θ_d = divergence angle

ν_r = angle between the vector to (x, y, z) and the z-axis

I. INTRODUCTION

The contrast in the shadow of a grating is observed to become weaker and eventually disappear as the distance between the grating and the surface on which the shadow appears is increased. This contrast reduction is a primary limitation of the shadow moire technique, a method used to measure extremely small variations or deformations in surfaces.

The contrast reduction is caused by the diffraction effect and the divergence effect. Diffraction is related to the interaction of light waves with the grating. Divergence is associated with the degree of collimation in the light beam.

The purpose of this thesis is to analyze the effect of diffraction and divergence on shadow contrast. In particular, the intensity patterns associated with each effect will be derived. The behavior of the contrast will be discussed. Also, the relationship between diffraction and divergence is presented. This knowledge will improve the versatility and usefulness of the shadow moire technique.

II. SHADOW MOIRE TECHNIQUE

The shadow moire technique is a current application of the phenomenon of moire fringes. Historically, the practical application of moire fringes began with Lord Rayleigh [1] who suggested in 1874 that this phenomenon could be used to judge the quality of gratings. In 1956, Guild [2] described the theory of moire fringes in detail and also discussed the use of moire patterns as a test of grating quality. More recently, the most important applications of grating moire patterns involve the use of shadow moire [3-5]. For a range of depth that is not too great, the shadow moire is ideal for measuring very small changes in the contours of surfaces such as deformations due to stress and strain. The applications involving contour measurements are a key interest in this study.

The contour measurements are made using the shadow moire technique. This technique produces a moire, or interference, pattern between a grating and the shadow of the grating as observed through the grating upon the surface of interest. The moire pattern identifies elevation contours along the surface. The technique has a limited range because the contrast of the shadow decreases with distance making the more distant contours difficult to observe.

The shadow moire technique is illustrated in Figure 1. A grating is placed above the surface of interest.
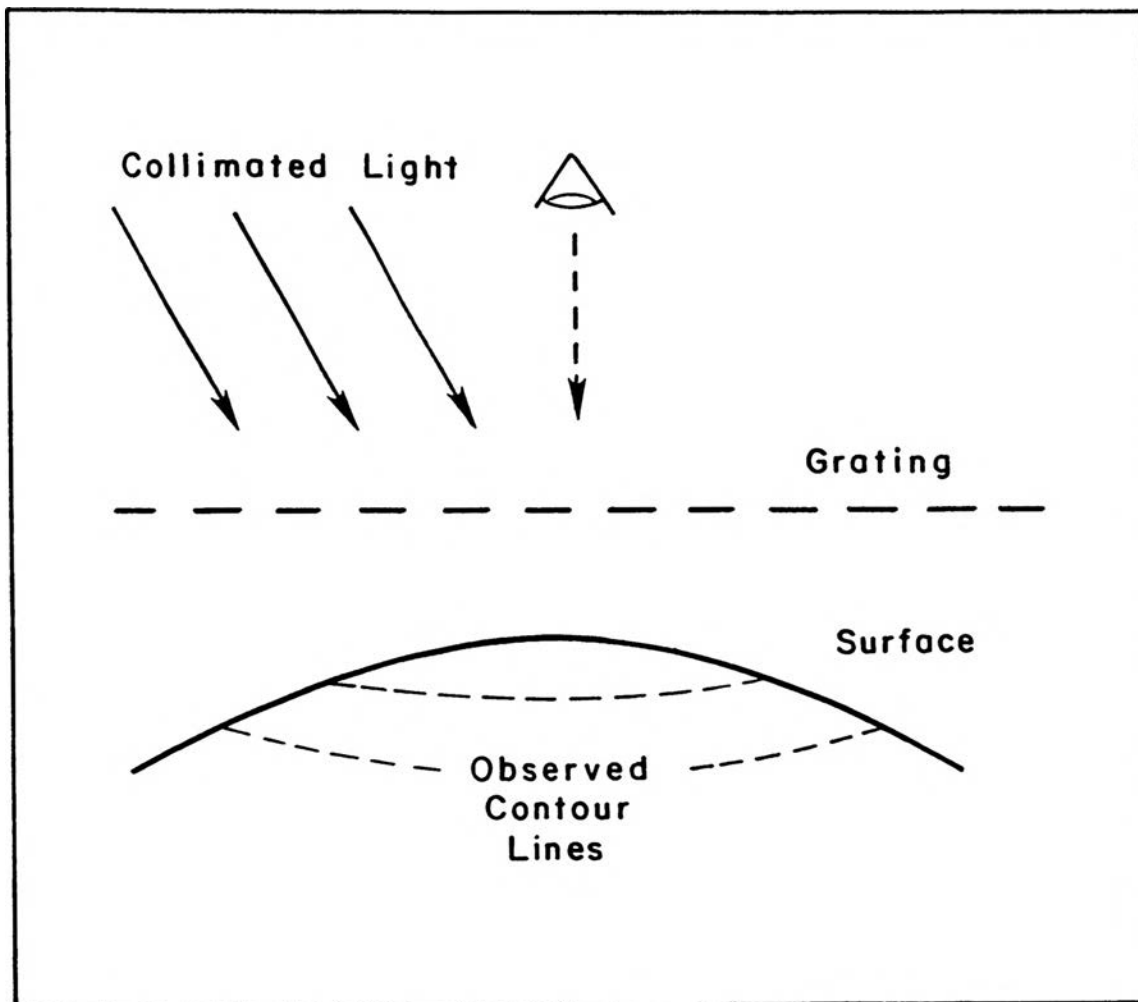
FIGURE 1. Shadow Moire Technique

The dashed lines represent the moire pattern between the grating and its shadow. These lines follow the contours of the surface.

Collimated light passes through the grating at a small
angle with respect to the normal of the grating plane. A
shadow of the grating is cast on the surface, but it is
distorted due to the variations in the surface. When the
surface is observed normally as shown, the interference
pattern between the grating and the distorted shadow
determines a contour map of the surface. In a typical
stress measurement, the contours are compared for the
surface under different levels of stress to measure the
deformations.

An example of the results of the moire technique is
shown in Figure 2. The contour fringes are used to deter-
mine the shape of a thermal contact switch. (The actual
length of the switch is approximately one-half inch.) The
grating lines and the interference pattern are clearly
visible. Each contour line corresponds to a surface
displacement of about three-thousandths of an inch with
respect to the plane of the grating.

A point of interest in Figure 2 is the variation in
shadow contrast. When the shadow contrast is low, the
resulting moire pattern also has low contrast. The shadow
contrast decreases as the distance between the grating and
the surface is increased. The contrast of the moire
pattern is lower at the bottom of the figure where the
switch surface is farther from the grating.

The purpose of this thesis is to give a quantitative
explanation for these contrast variations. Part of the
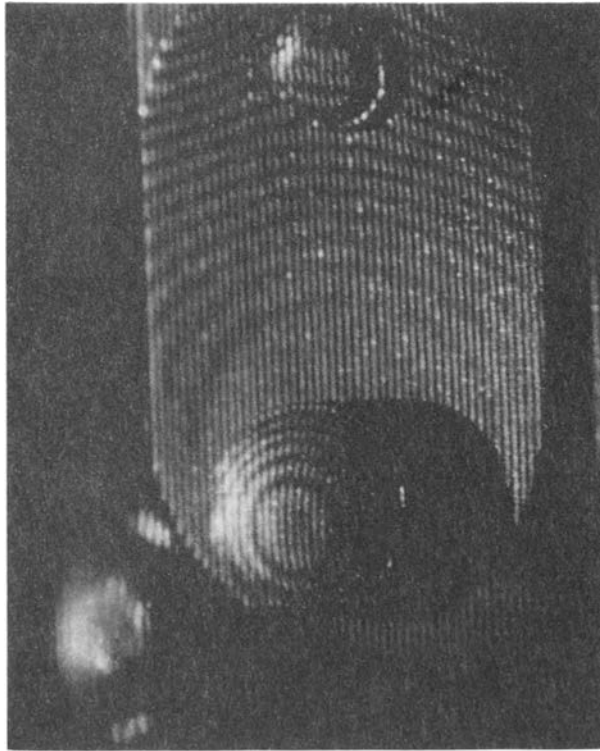
FIGURE 2. Example of a Shadow Moire

The contour lines of a thermal contact switch are obtained using the shadow moire technique.

explanation results from diffraction, that is the interaction of light waves with the grating. The explanation also must include divergence effects which depend on the collimation of the incident light. In both cases, a mathematical description predicts the contrast variation with distance and shows how the phenomenon scales with grating size.

III. DIFFRACTION

As previously discussed, the reduction of contrast in the intensity pattern behind a grating is caused in part by diffraction effects, i.e. the wave nature of light. In order to predict the diffraction effect, the Huygens-Fresnel principle can be used [6,7]. This principle states that each point on a wave front can be considered a point source. The propagation of the wave is found from the superposition of the waves from each of the point sources. This approach is valid to the extent that the vector nature of light can be ignored [8]. If a light wave is incident on an aperture, the illumination behind the aperture is found by considering the contributions from the point sources in the aperture. Thus, the light spreads out and "smears" the aperture shadow. Hence, the contrast of the shadow is reduced. In what follows, the field behind a grating, i.e. the aperture, will be mathematically calculated using the Huygens-Fresnel principle. The contrast of the shadow will be discussed and a scaling law will be derived.

A. INTENSITY

The intensity pattern to be found is for the binary grating shown in Figure 3. The shaded region has zero transmittance (i.e. it is completely opaque) and the unshaded slits have a transmittance of one (i.e. the slits
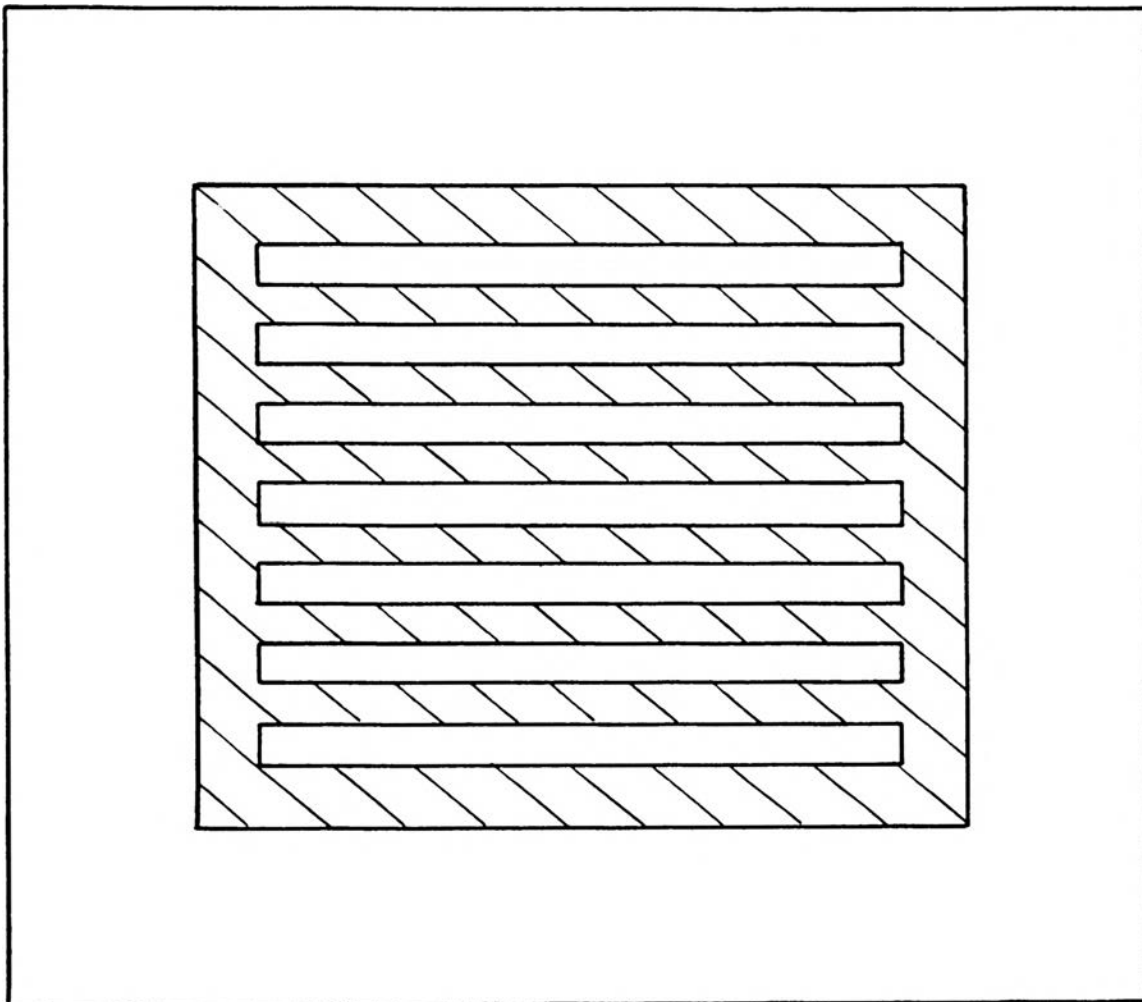
FIGURE 3. Binary Grating

    A binary grating has a transmittance that is either one or zero which is indicated by the unshaded and shaded regions, respectively.

are transparent lossless regions). For the purposes of this analysis, the widths of the transparent and opaque strips are equal. The illumination will be a unit amplitude plane wave parallel to the plane of the grating.

The fields, or waves, in this section are mathematically expressed as complex-valued scalars (often called phasors) which denote the amplitude and phase of the waves. In the case of a linearly polarized wave, the field may be regarded as either the electric or the magnetic field strength. This convention is implicit in scalar diffraction theory.

The field behind the grating, U, is found by the mathematical statement of the Huygens-Fresnel principle:

$$U(x,y) = \iint_{-\infty}^{\infty} G(\tau,\beta)h(x-\tau,y-\beta)d\tau d\beta \qquad (1)$$

where $G(x,y)$ = product of the incident field and the grating transmittance function

$h(x,y)$ = field from the heuristic point sources.

The plane of the grating is assumed to be the z = 0 plane. Also, the field $h(x,y)$ is given explicitly by

$$h(x,y) = \frac{1}{j\lambda r} \exp(jkr)\cos(\nu r)$$

where $\cos \nu_r$ = directivity factor

ν_r = angle between the vector to the point (x,y,z) and the z-axis

$r = \sqrt{x^2 + y^2 + z^2}$.

Since field quantities are used, the convolution in Equation (1) accounts for the interference that occurs between the various point sources.

In the region of Fresnel diffraction, the equation becomes

$$U(x,y) = \frac{1}{j\lambda z} \exp(jkz) \iint_{-\infty}^{\infty} G(\tau,\beta)$$

$$\cdot \exp\{j \frac{k}{2z} [(x-\tau)^2+(y-\beta)^2]\}d\tau\,d\beta \qquad (2)$$

where λ = wavelength

$k = \frac{2\pi}{\lambda}$ = wave number.

The assumptions to this point are that the grating period is much greater than λ, that z is much greater than the grating period, and that the Fresnel approximation holds. Equation (2) can be expressed as

$$U(x,y) = \frac{1}{j\lambda z} \exp(jkz)\exp[j \frac{\pi}{\lambda z} (x^2+y^2)]$$

$$\cdot F\{G(\tau,\beta)\exp[j \frac{k}{2z} (\tau^2+\beta^2)]\}_{\frac{x}{\lambda z},\frac{y}{\lambda z}} \qquad (3)$$

where $F\{\ \}_{f_1,f_2}$ represents the two-dimensional Fourier transform in the variables f_1 and f_2. The detailed development of Equation (3) from the Huygens-Fresnel principle is given by Goodman [9].

The function G becomes the grating transmittance function g if the illumination is a unit-amplitude, normally incident plane wave. The function g is mathematically a pulse train in the x-direction and unity in the

y-direction. Representing the pulse train by its Fourier series,

$$g(x,y) = \frac{1}{2} + \frac{2}{\pi} \sum_{n=1}^{\infty} \frac{(-1)^{n+1}}{(2n-1)} \cos[2\pi x(2n-1)/p] \quad (4)$$

where p is the grating period.

The substitution of Equation (4) into Equation (3) requires the solution of

$$F\{m \cos(2\pi f\tau)\exp[j\,\frac{k}{2z}\,(\tau^2+\beta^2)]\}_{\frac{x}{\lambda z},\frac{y}{\lambda z}}$$

$$= F\{m \cos(2\pi f\tau)\exp(j\,\frac{k}{2z}\,\tau^2)\}_{\frac{x}{\lambda z}} F\{\exp(j\,\frac{k}{2z}\,\beta^2)\}_{\frac{y}{\lambda z}}$$

$$= F\{m \cos(2\pi f\tau)\}_{\frac{x}{\lambda z}} *F\{\exp(j\,\frac{k}{2z}\,\tau^2)\}_{\frac{x}{\lambda z}}$$

$$\cdot F\{\exp(j\,\frac{k}{2z}\,\beta^2)\}_{\frac{y}{\lambda z}}$$

Evaluating the transforms give

$$\{\frac{m}{2}[\delta(\frac{x}{\lambda 2}-f)+\delta(\frac{x}{\lambda z}+f)]*[j\lambda z\,\exp(-j\,\frac{\pi}{\lambda z}\,x^2)]\}\exp(-j\,\frac{\pi}{\lambda z}\,y^2)$$

$$= (j\lambda zm/2)\{\exp[-j\,\frac{\pi}{\lambda z}\,(x^2+y^2)]+\exp[-j\,\frac{\pi}{\lambda z}\,(x+f\lambda z)^2]\}$$

$$\cdot \exp(-j\,\frac{\pi}{\lambda z}\,y^2)$$

$$= (j\lambda zm)\exp[-j\,\frac{\pi}{\lambda z}\,(x^2+y^2)][\cos(2\pi xf)$$

$$\cdot \exp(-j\pi\lambda zf^2)]. \quad (5)$$

The following transform is also required.

$$F\{m \exp[j\,\frac{k}{2z}\,(\tau^2+\beta^2)]\}_{\frac{x}{\lambda z},\frac{y}{\lambda z}} = (j\lambda zm)\exp[-j\,\frac{\pi}{2z}\,(x^2+y^2)]. \quad (6)$$

The diffracted field is found by substitution of Equation (4) into Equation (3). Since the transform of the sum of the terms is the sum of the transforms of the terms,

$$U(x,y) = \frac{1}{j\lambda z} \exp(jkz)\exp[j\frac{\pi}{\lambda z}(x^2+y^2)]\{j\frac{\pi}{\lambda z}\exp[-j\frac{\pi}{\lambda z}$$

$$\cdot(x^2+y^2)]+\frac{2}{\pi}\sum_{n=1}^{\infty}(j\lambda z)\frac{(-1)^{n+1}}{(2n-1)}\exp[-j\frac{\pi}{\lambda z}(x^2+y^2)]$$

$$\cdot \exp[-j\pi\lambda z(2n-1)^2/p^2]\cos[2\pi x(2n-1/p)]\}$$

$$= \frac{1}{2}\exp(jkz)\{1+\frac{4}{\pi}\sum_{n=1}^{\infty}\frac{(-1)^{n+1}}{(2n-1)}\exp[-j\pi\lambda z(2n-1)^2/p^2]$$

$$\cdot \cos[2\pi x(2n-1)/p]$$

$$= \frac{1}{2}\exp(jkz)\{1+\frac{4}{\pi}\sum_{n=1}^{\infty}\frac{(-1)^{n+1}}{(2n-1)}\cos[\pi\lambda z(2n-1)^2/p^2]$$

$$\cdot \cos[2\pi x(2n-1)/p]+j\frac{4}{\pi}\sum_{n=1}^{\infty}\frac{(-1)^{n+1}}{(2n-1)}$$

$$\cdot \sin[\pi\lambda z(2n-1)^2/p^2]\cos[2\pi x(2n-1)/p]. \quad (7)$$

Note that z is the distance behind the grating. Also, the grating is assumed to be infinite. The effects of a finite aperture are negligible if the grating size is very much larger than the grating period.

The intensity is

$$I(x,y) = C|U|^2 = C\{\frac{1}{2}+\frac{2}{\pi}\sum_{n=1}^{\infty}\frac{(-1)^{n+1}}{(2n-1)}\cos[\pi\lambda z(2n-1)^2/p^2]$$

$$\cdot \cos[2\pi x(2n-1)/p]\}^2+C\{\frac{2}{\pi}\sum_{n=1}^{\infty}\frac{(-1)^{n+1}}{(2n-1)}$$

$$\cdot \sin[\pi\lambda z(2n-1)^2/p^2]$$

$$\cdot \cos[2\pi x(2n-1)/p]\}^2. \quad (8)$$

where C is a constant. The constant C will be dropped in what follows since the relative intensity distribution is of interest rather than the absolute value.

The Fresnel intensity pattern has the property that it is periodic in z with a period $2p^2/\lambda$. Hence, the grating is imaged for $z = 2mp^2/\lambda$ where $m = 1,2,3,...$ (In a physical situation, the absolute intensity will decrease for increasing z.) This self-imaging property of gratings is known as the Talbot effect and has been observed by Lord Rayleigh [10] and Montgomery [11]. In fact, a real-time range measurement technique is based on the Talbot effect [12]. The Fresnel pattern also has been verified between the self-imaging planes [13].

The intensity pattern is shown in Figure 4 for the three different cases. The transmittance function of the grating is

$$g(x,y) = \frac{1}{2} + \frac{2}{\pi} \sum_{n=1}^{\infty} \frac{(-1)^{n+1}}{(2n-1)}\cos[2\pi x(2n-1)/p] \qquad (9)$$

The first curve displays the intensity directly behind the grating which is

$$I(x,y) = g^2(x,y) \qquad (10)$$

Recall that a unit amplitude plane wave is the incident field and the C has been dropped. Note that the contrast ratio, or the ratio of the maximum intensity to the minimum intensity, is infinity. The second curve is obtained from Equation (8) when z equals $p^2/4\lambda$. The intensity becomes
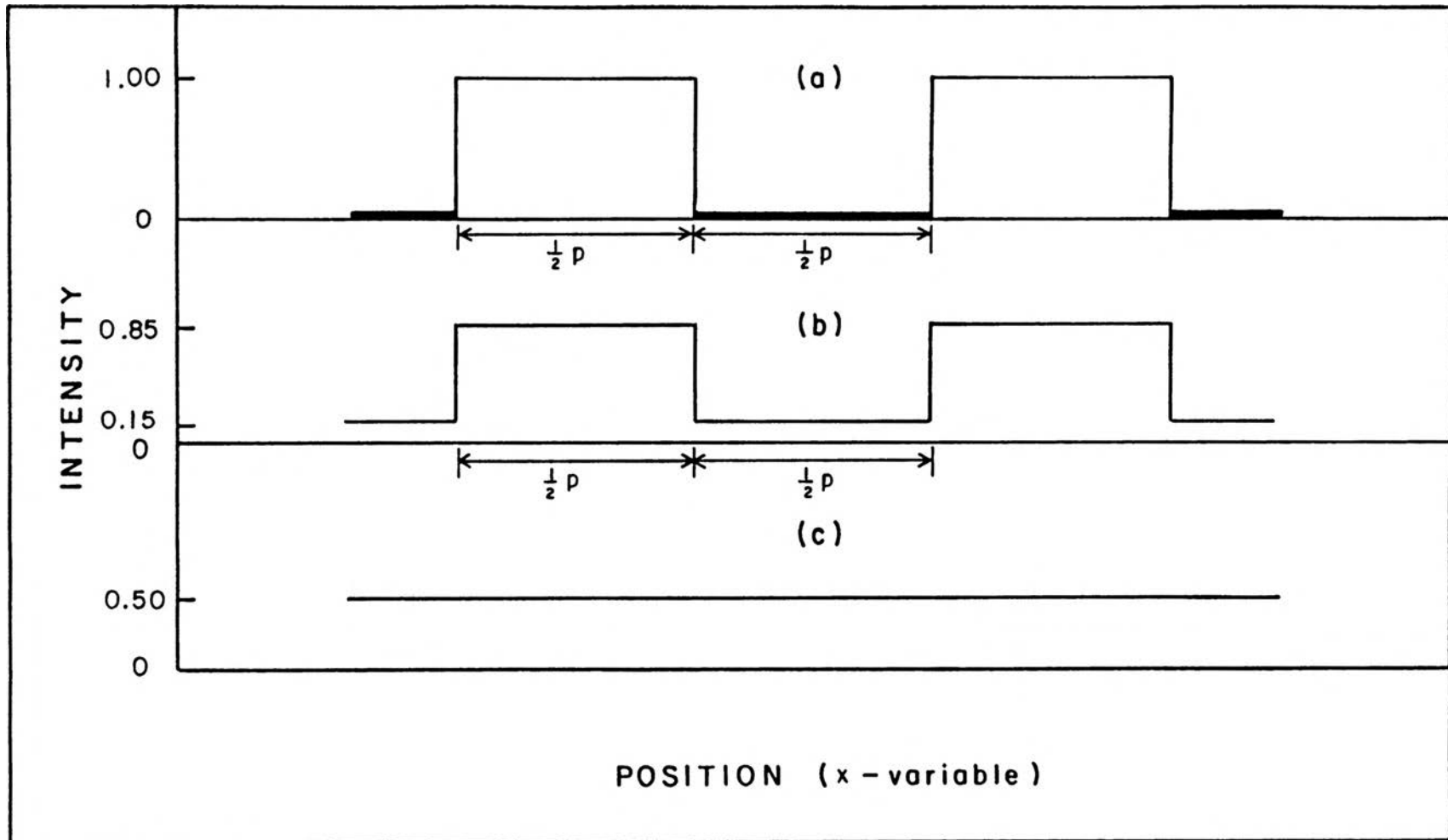
FIGURE 4. Diffraction Intensity Patterns

The intensity pattern as a function of x is shown (a) directly behind the grating (i.e. $z = 0^+$), (b) at a distance $z = p^2/4\lambda$, and (c) at a distance $z = p^2/2\lambda$.

$$I(x,y) = \left| \frac{1}{2} + \frac{2}{\pi} \sum_{n=1}^{\infty} \frac{(-1)^{n+1}}{(2n-1)} \left(\frac{1}{\sqrt{2}} \right) \cos[2\pi x(2n-1)/p] \right.$$

$$\left. + j \frac{2}{\pi} \sum_{n=1}^{\infty} \frac{(-1)^{n}}{(2n-1)} \left(\frac{1}{\sqrt{2}} \right) \cos[2\pi x(2n-1)/p] \right|^2$$

$$= \left| \left[\frac{1}{2} - \frac{1}{2\sqrt{2}} + \frac{1}{\sqrt{2}} g(x,y) \right] + j \left[\frac{1}{2\sqrt{2}} - \frac{1}{\sqrt{2}} g(x,y) \right] \right|^2$$

$$= \begin{cases} 0.8536 & g(x,y) = 1 \\ \\ 0.1464 & g(x,y) = 0 \end{cases} \tag{11}$$

The contrast ratio is 5.8287. The last curve displays the intensity when z equals $p^2/2\lambda$. Equation (8) gives

$$I(x,y) = \left| \frac{1}{2} + j\frac{2}{\pi} \sum_{n=1}^{\infty} \frac{(-1)^{n}}{(2n-1)} (1)\cos[2\pi x(2n-1)/p] \right|^2$$

$$= \left| \frac{1}{2} + j\left[\frac{1}{2} - g(x,y) \right] \right|^2$$

$$= 0.50 \quad \text{everywhere.} \tag{12}$$

The contrast ratio is unity. Note the phase of the wave-front varies in the observation plane, but the intensity is constant.

The curves in Figure 4 are intended to show when the shadow completely disappears and roughly how the contrast decreases. The choices of z in Figure 4(b) and (c) greatly simplify the shape of the curves. In general, the intensity will vary rapidly as a function of x.

The contrast ratio is emphasized above because it is a useful measure of how well the shadow can be observed. The difference between maximum intensity and minimum intensity will vary with the amplitude of the incident wave. The

relative intensities in the pattern are independent of the amplitude.

The previous analysis is done for light of a single wavelength. The results can be extended to the situation in which the illumination is incoherent and consists of many frequencies. The incoherence eliminates the effects of interference between the light of different wavelengths. Thus, the resulting intensity is the summation of the intensities associated with each wavelength.

B. SCALING LAW

The intensity pattern due to diffraction has a squared scaling law. Consider the intensity pattern at a specified distance from a grating. A similar pattern occurs at N^2 the original distance, if the grating size is increased by the factor N. Therefore, the diffraction pattern is known in general if it is known for a single grating. This scaling law was demonstrated by Arkadiew [14] and is more recently described by Sommerfeld [15].

The scaling law is apparent from Equation (8) which is

$$I(x,y) = \{\frac{1}{2} + \frac{2}{\pi} \sum_{n=1}^{\infty} \frac{(-1)^{n+1}}{(2n-1)} \cos[\pi\lambda z(2n-1)^2/p^2]$$
$$\cdot \cos[2\pi x(2n-1)/p]\}^2 + \{\frac{2}{\pi} \sum_{n=1}^{\infty} \frac{(-1)^{n+1}}{(2n-1)}$$
$$\cdot \sin[\pi\lambda z(2n-1)^2/p^2]\cos[2\pi x(2n-1)/p]\}^2.$$

Let the grating size be increased by the factor N (i.e. replace p with Np). The x and y coordinates must also be

increased by N since the scaled pattern will increase by the factor N. The arguments of the second and third cosine factors include the ratio x/p. Thus, the arguments are unchanged. The arguments of the remaining sinusoidal terms include the ratio z/p^2. Therefore, the distance z must be increased by N^2 to maintain the same argument and a similar intensity pattern.

IV.   DIVERGENCE

The reduction of contrast in the intensity pattern behind a grating can be caused by the divergence of the illuminating light.   A light beam is said to diverge if its rays are not parallel.   The extent of the beam divergence is specified by the divergence angle θ_d.   This angle is ideally the maximum angle a light ray in the beam can have with respect to the beam axis.   The model of the beam thus consists of rays which have angles uniformly ranging from zero to the divergence angle.   Geometrical optics predicts the effect of such a beam normally incident on a grating. A geometrical approach is used since the ray behavior of light is of interest here.   The portion of the beam that is allowed through the grating still contains rays of every angle up to the divergence angle.   Light then propagates behind the opaque sections of the grating.   Hence, the contrast behind the grating is progressively reduced.   This geometrical approach coupled with a convolution technique gives a quantitative description of the intensity pattern. An explicit measure of the contrast is derived.   Also, the scaling law that is associated with the effect is shown.

A.   INTENSITY

The intensity pattern is found using the model shown in Figure 5.   The model consists of a light source, a binary grating, and an observation plane, proceeding from
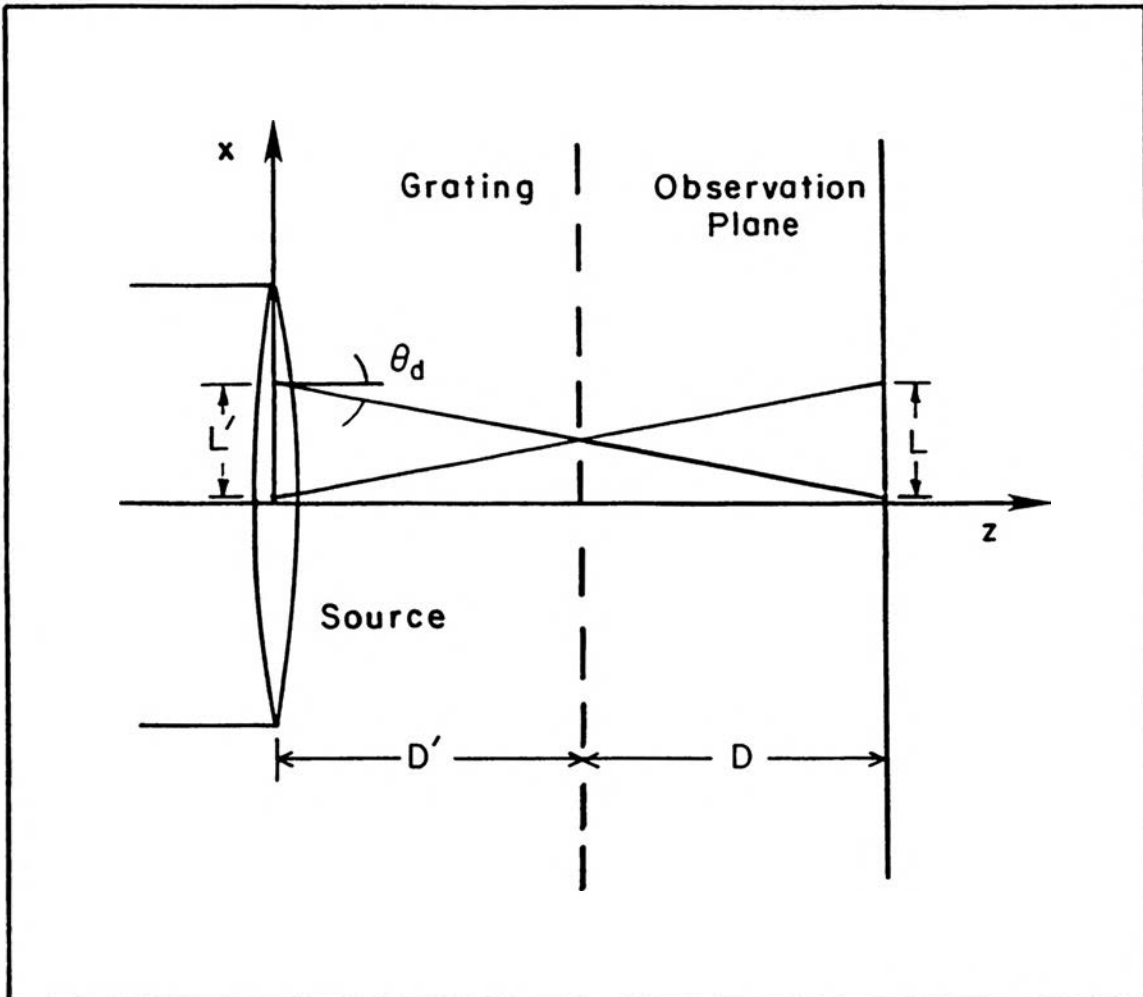
FIGURE 5. Illustration of the Divergence Effect

The impulse response of a point in the aperture is shown for the divergence effect.

left to right. Since the transmittance of the grating only varies in one direction (i.e. the x-direction), the analysis only needs to be carried out in the xz-plane. Note that the z-direction is the direction of propagation. The analysis will be confined to the region about the axis of propagation. Therefore, the effect of the finite size of the grating can be neglected.

The source produces white light which will be characterized by a small divergence angle

$$\theta_d << 1. \tag{1}$$

Since the light is incoherent, the analysis can be carried out for each frequency separately. The total intensity in the observation plane will be the summation of the intensities due to each frequency.

The effect of diffraction will be assumed negligible. A later section will discuss what relationship must exist between the divergence angle, the wavelength of light, and the grating period for this assumption to be valid.

The grating is perpendicular to the axis of propagation and is a distance D' from the source. Once again for mathematical simplicity, the widths of the opaque and transparent strips will be assumed equal. The grating period will be given by p.

The observation plane is a distance D behind the grating and is parallel to the plane of the grating.

The convolution approach is a consequence of the following treatment. Select a point in one of the transparent strips near the axis. From the definition of the divergence angle, all of the light rays passing through that point must come from a circle of diameter L' centered directly in front of the point. As previously discussed, the analysis only needs to be carried out in the xz-plane. Hence, the rays passing through the selected point comes from a length L' of a line source. By the geometry shown in Figure 5,

$$L' = 2D' \tan \theta_d \approx 2D'\theta_d \quad \text{for } \theta_d << 1. \tag{2}$$

If the source length is smaller than this L', then the source width determines an effective divergence angle θ_d'.

$$\theta_d' = \tan^{-1}[(\text{source length})/2D']$$

The former case will be assumed in the following treatment. (If the latter case occurs, the source length should be substituted for L' and θ_d' for θ_d.)

The rays going through the selected point illuminate a length L in the observation plane. (Recall that only the x-coordinate is of interest in the observation plane.) As in Equation (2),

$$L = 2D \tan \theta_d \approx 2D\theta_d. \tag{3}$$

Combining Equations (2) and (3) gives

$$L = D(L'/D'). \tag{4}$$

Thus, L depends linearly on the distance to the observation plane.

The illumination of length L in the observation plane will be henceforth referred to as the spot. Also, for mathematical simplicity the intensity everywhere in this spot will be considered uniform.

The spot is the impulse response of the grating. Each point of the grating which has a transmittance of unity produces such a spot in the observation plane. The final intensity pattern is the summation of these spots, that is the convolution of the impulse response with the grating transmittance function [16].

Mathematically, the grating is represented by a pulse train (i.e. the spatial transmittance function)

$$g(x) = \sum_{n=-\infty}^{\infty} \text{rect}\left[\frac{x-np}{(p/2)}\right] . \tag{5}$$

The impulse response of the grating is a single pulse

$$h(x) = A \, \text{rect}(\frac{x}{L}). \tag{6}$$

The amplitude of the impulse response A (i.e. the intensity of the spot) depends on the source and the distance D. If the amplitude is A_o at a distance D_o behind the grating, the amplitude elsewhere is given by

$$A = A_o D_o / D. \tag{7}$$

The intensity of a single spot is inversely proportional to D because a constant energy per unit length in the y-direction is distributed over L. Recall that L is proportional to D by Equation (4). Note that the stated conditions allow the source and grating to be considered infinite in the y-direction. The intensity is

$$I(x) = g(x)*h(x) = \int_{-\infty}^{\infty} g(\tau)h(x-\tau)d\tau. \tag{8}$$

The conditions of operating near the axis and using incoherent light are necessary so that the system can be considered linear and spatially-invariant. Linearity allows the "summation of spots" (i.e. superposition); invariance means that h(x) does not change for different points in the grating aperture.

The result of the convolution is shown in Figure 6 for three different cases. The first curve is valid when the spot length, L, is less than the width of the transparent strips, $\frac{1}{2}$ p. That is,

$$L = m(\frac{1}{2} p) \quad \text{for} \quad 0 < m \leq 1. \tag{9}$$

Note that the contrast ratio or the ratio of maximum intensity to minimum intensity is infinity. The shadow can easily be seen. The second curve is valid when

$$L = m(\frac{1}{2} p) \quad \text{for} \quad 1 \leq m \leq 2. \tag{10}$$

Here the contrast ratio is finite except when L equals $\frac{1}{2}$ p (i.e. m = 1). The shadow becomes progressively harder to
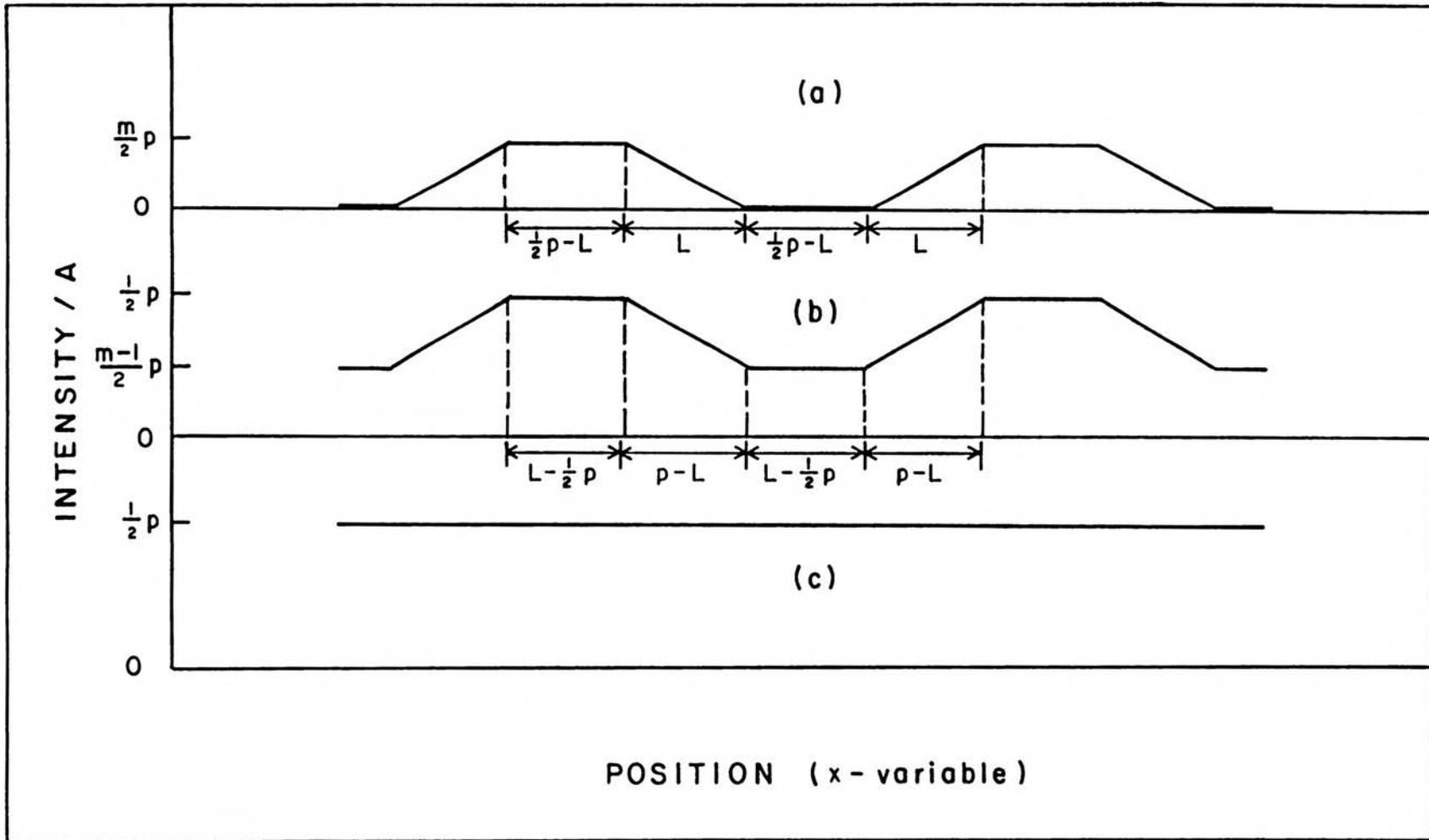
FIGURE 6. Divergence Intensity Patterns

The intensity pattern as a function of x is shown (a) where $L = m(\frac{1}{2}p)$, $0 < m \leq 1$; (b) where $L = m(\frac{1}{2}p)$, $1 \leq m \leq 2$; and (c) where $L = \frac{1}{2}p$.

detect. The final curve is valid when L precisely equals the grating spacing. There is no variation in the intensity and the contrast ratio is unity. The shadow structure has disappeared.

B. CONTRAST

The presence of a shadow from the grating is detected by the contrast in the intensity pattern. The contrast ratio, C.R., has a closed form for the divergence effect. In the previous section, the contrast ratio was shown to be finite only when (see Equation (10))

$$L = m(\tfrac{1}{2} p) \quad \text{for} \quad 1 < m \leq 2.$$

The curve in Figure 6(b) corresponds to this condition. Here the maximum intensity is

$$I_{max} = A(\tfrac{1}{2} p).$$

The minimum intensity is

$$I_{min} = A[(m-1)(\tfrac{1}{2} p)] = A[L - (\tfrac{1}{2} p)].$$

The contrast ratio is

$$C.R. = I_{max}/I_{min} = (\tfrac{1}{2} p)/[L - (\tfrac{1}{2} p)]$$
$$= 1/(2L/p - 1). \tag{11}$$

Using Equation (3), the contrast ratio can be expressed in terms of measurable quantities--the divergence angle, the distance D, and the grating period.

$$C.R. = 1/(4\theta_d D/p - 1). \tag{12}$$

This equation is valid for

$$1 \leq C.R. < \infty.$$

The curves in Figure 7 are an example. The calculations were done for divergence angles of 0.0072 radians, 0.0060 radians, 0.0048 radians, and 0.0036 radians. For the curve with θ_d equal to 0.0048 radians, the contrast ratio approaches infinity as the ratio D/p approaches 52.1. When D/p equals 104.2, the contrast ratio is unity.

C. SCALING LAW

The divergence effect scales linearly, whereas the diffraction effect was shown to have a squared scaling law. If the size of the grating is changed by a factor, a similar intensity pattern will result for the distance D changed by the same factor.

This property can be seen through the convolution results in Figure 6. The curves are derived for (Equations (9) and (10))

$$L = m(\tfrac{1}{2} p).$$

If the size of the grating is increased by N, similar patterns occur for

$$NL = m(\tfrac{1}{2} Np).$$
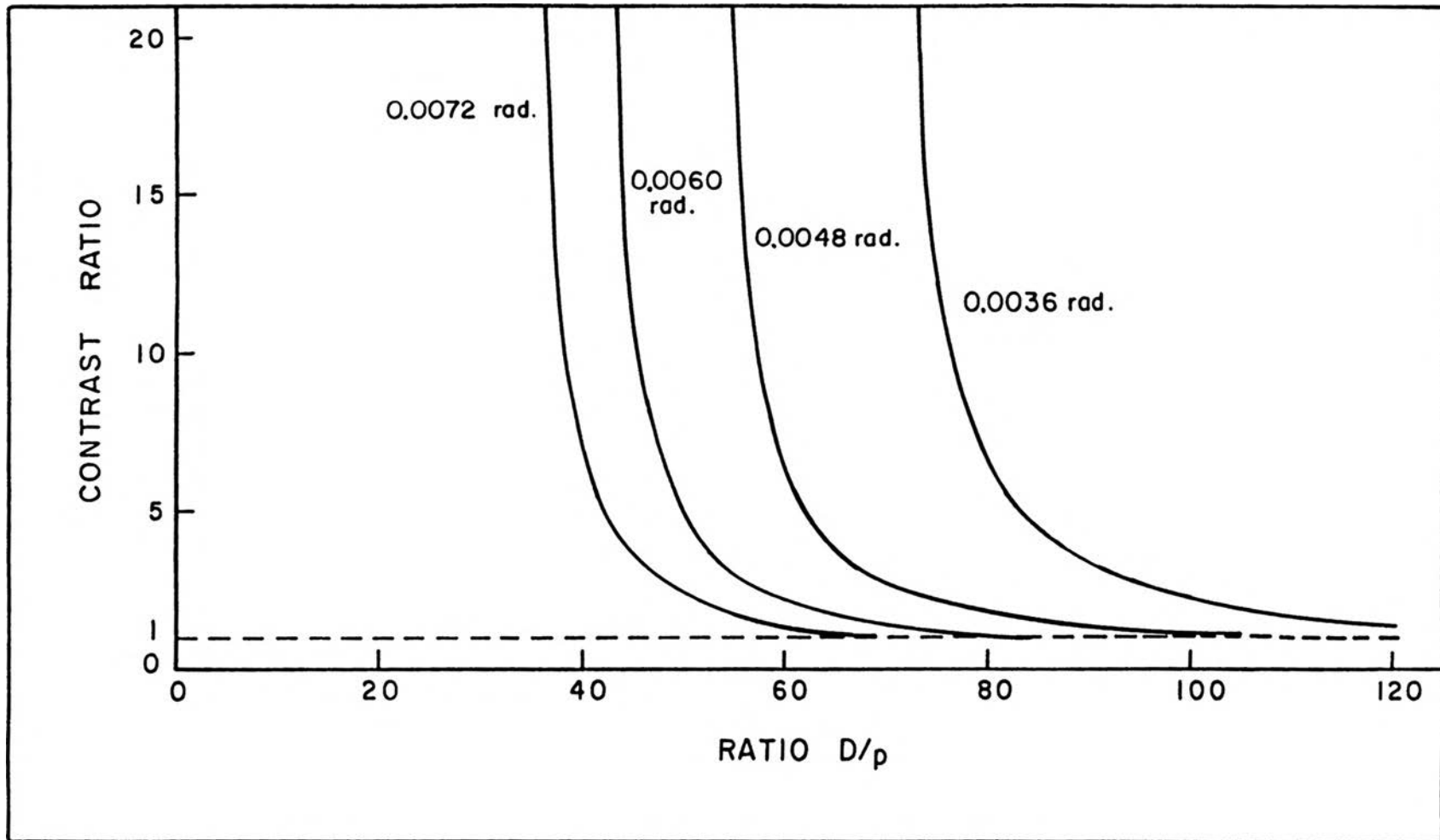
FIGURE 7.   Contrast Ratio vs. D/p

The contrast ratio as a function of the ratio D/p is shown for divergence angles of 0.0072 radians, 0.0060 radians, 0.0048 radians and 0.0036 radians.

But L is proportional to D by Equation (4). Thus, the new distance is ND.

The scaling law can also be seen from the contrast ratio formula, Equation (12),

$$C.R. = 1/(4\theta_d D/p - 1).$$

The contrast ratio is identical if the ratio D/p is a constant.

V. EXPERIMENT

An experimental investigation of the effect of the
divergence is presented. The importance of diffraction is
widely appreciated for optical gratings, but the signifi-
cance of divergence is not widely appreciated. Thus, the
previous theoretical results for divergence are experimen-
tally verified in regard to the contrast ratio and the
linear scaling law.

A. PROCEDURE

The experiment was set up according to the model
discussed in Section IV. A white light source illuminated
a grating normally. The resulting intensity pattern was
measured in various planes behind the grating. An incan-
descent lamp was used as the source. The light was colli-
mated to a divergence angle of not more than 0.0090 ra-
dians. Note that 0.0090 is much less than one as desired.
The distance to the grating was such that the width of the
beam did not effect the data.

Four different gratings were used. The spatial
periods are one-half inch per line, three-eighths inch per
line, one-fourth inch per line, and one-eighth inch per
line. The opaque and transparent strips are equal in
width.

For each grating, the maximum intensity and minimum
intensity were measured in a series of planes behind the

grating. The average maximum intensity and average minimum intensity were determined for each plane close to the axis of the system. This data was combined to form the contrast ratio.

The experiment was designed so that the diffraction effects were negligible. A measure of how fast the light spreads behind the grating in the divergence case is the divergence angle. This angle was on the order of 0.0090 radians. In the diffraction case, the comparable measure is the first order diffraction angle which equals the wavelength divided by the grating period. The largest first order diffraction angle was 0.22 milliradians. Since the divergence angle is more than an order of magnitude greater than the first order diffraction angle, divergence is the dominant effect. A more complete discussion of these quantities will be given in Section VI.

B. DATA ANALYSIS

The contrast ratio data is given in Figure 8. A curve is shown for each of the gratings used. As expected, the contrast ratio is initially infinite. It smoothly de-creases to one as the observation distance is increased. Recall that the intensity is uniform (i.e. no shadow) when this ratio is unity.

A ready verification of the effect producing the variation in contrast is found in the scaling relationship which holds. The divergence effect obeys a linear scaling
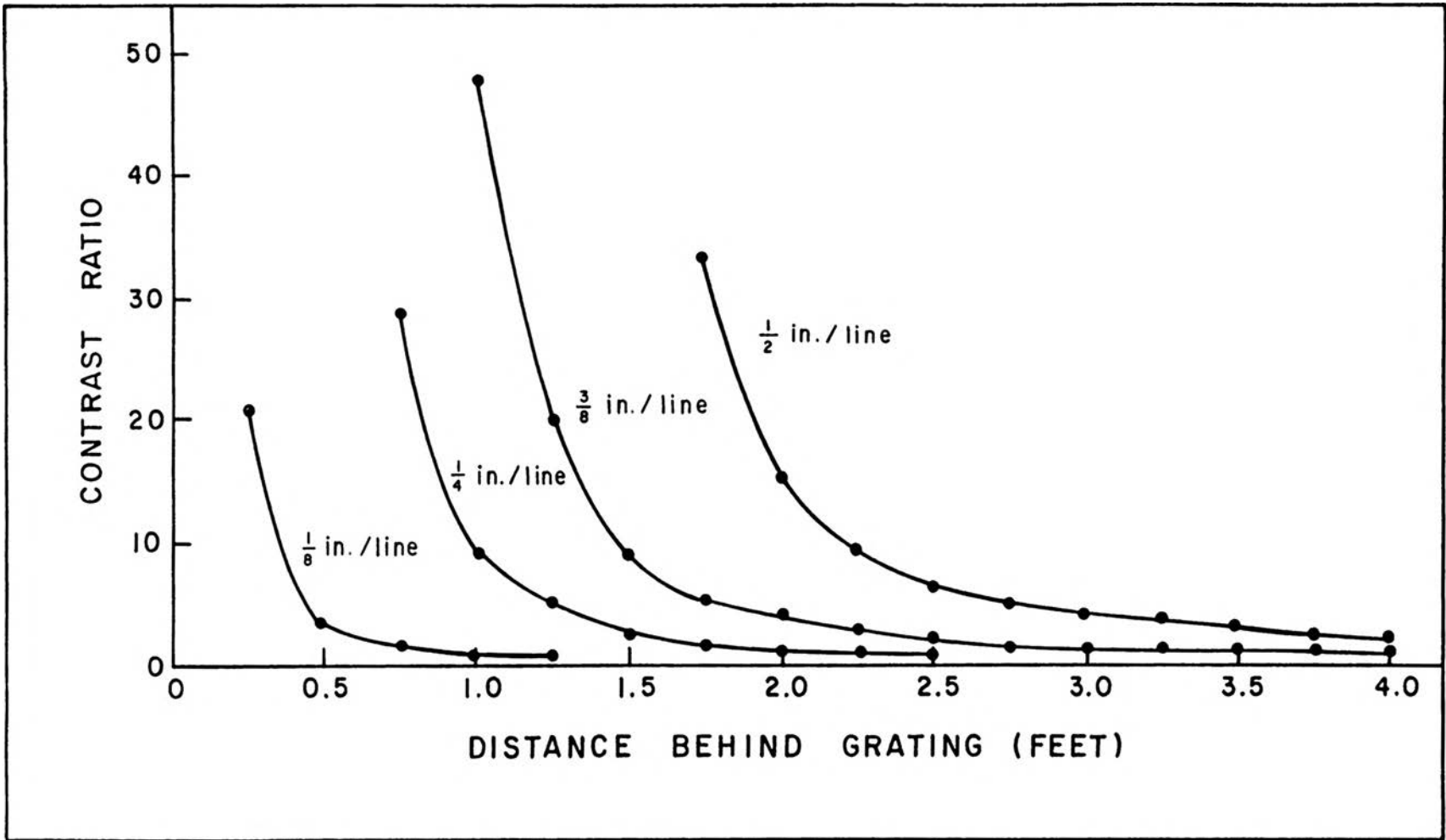
FIGURE 8. Contrast Ratio vs. Distance

The contrast ratio as determined by experiment is shown as a function of distance for various sizes of gratings.

law. The diffraction effect obeys a squared scaling law.
Figure 9 shows the same data linearly scaled. The data
points closely agree as a function of the distance divided
by the grating period. This agreement clearly shows that
divergence is the dominant effect.

The scaled data is also compared to the theoretical
contrast ratio in Figure 9. The contrast ratio is given by
the Equation (12) in Section IV.

$$C.R. = 1/(4\theta_d D/p - 1) \hspace{3cm} (1)$$

The given curve is calculated for a divergence angle of
0.0048 radians. This particular divergence angle is used
since it most closely matches the experimental data. The
data approaches infinity when D/p is on the order of 45.
The formula goes to infinity as D/p approaches 52.1. The
data is approximately one when D/p roughly equals 110. The
formula is unity when D/p equals 104.2.

The experimental divergence angle of 0.0048 radians is
also of the same order of magnitude as the estimated
divergence angle of 0.0090 radians.

The data and the theoretical formula coincide even
more closely if background light is taken into account.
Unfortunately, the background light could not be eliminated
during the experiment. To approximate this factor, assume
that the background intensity was equal to ten percent of
the actual maximum intensity when D/p was equal to 75.
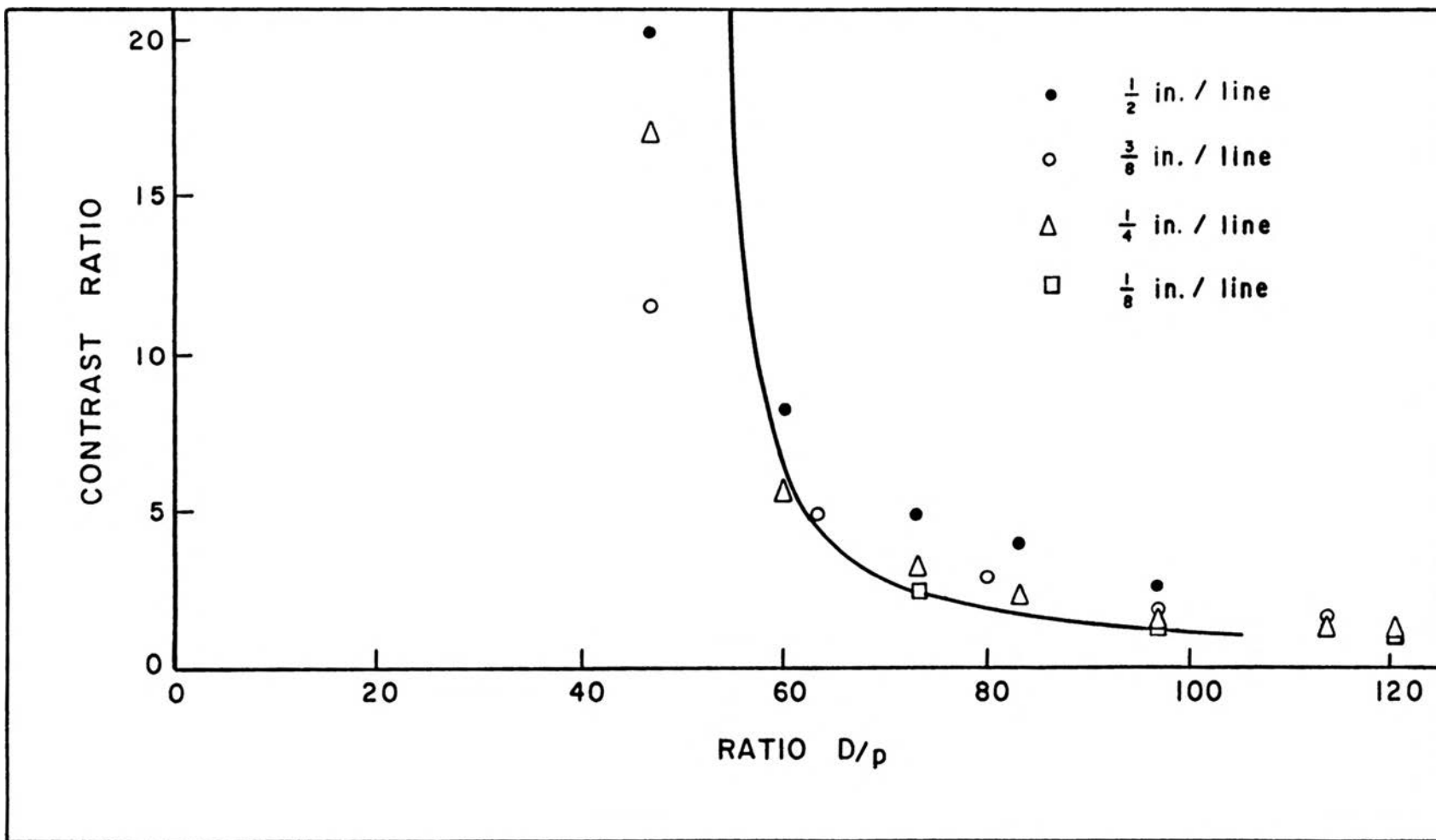From Figure 6 and Equation (7) in Section IV,

FIGURE 9.   Scaled Contrast Ratio

The contrast ratio is shown as a function of the ratio D/p for various gratings and is compared to the theoretical result.

$$I_{max} = (75A_op/D)(\tfrac{1}{2} p)$$

and

$$I_{min} = (75A_op/D)[L-(\tfrac{1}{2} p)]$$

where D_o/p is set equal to 75. The measured intensities are then

$$I'_{max} = (75A_op/D)(\tfrac{1}{2} p)+(0.1)(75A_op/D)(\tfrac{1}{2} p)$$

and

$$I'_{min} = (75A_op/D)[L-(\tfrac{1}{2} p)]+(0.1)(75A_op/D)(\tfrac{1}{2} p).$$

The contrast ratio becomes

$$C.R. = I'_{max}/I'_{min} = [1+0.1(75)^{-1}D/p]/\{[4\theta_d + 0.1(75)^{-1}]D/p-1\} \tag{2}$$

Figure 10 shows the resulting curve for θ_d equal to 0.0048 radians. Note that the curve fits the data better for low values of D/p. Equation (2) approaches infinity as D/p approaches 48.7 whereas Equation (1) does so as D/p approaches 52.1. Both equations equal unity at 104.2.

The agreement of the data to the contrast ratio formula and the estimated divergence angle serve as additional verification of the dominance of the divergence effect.
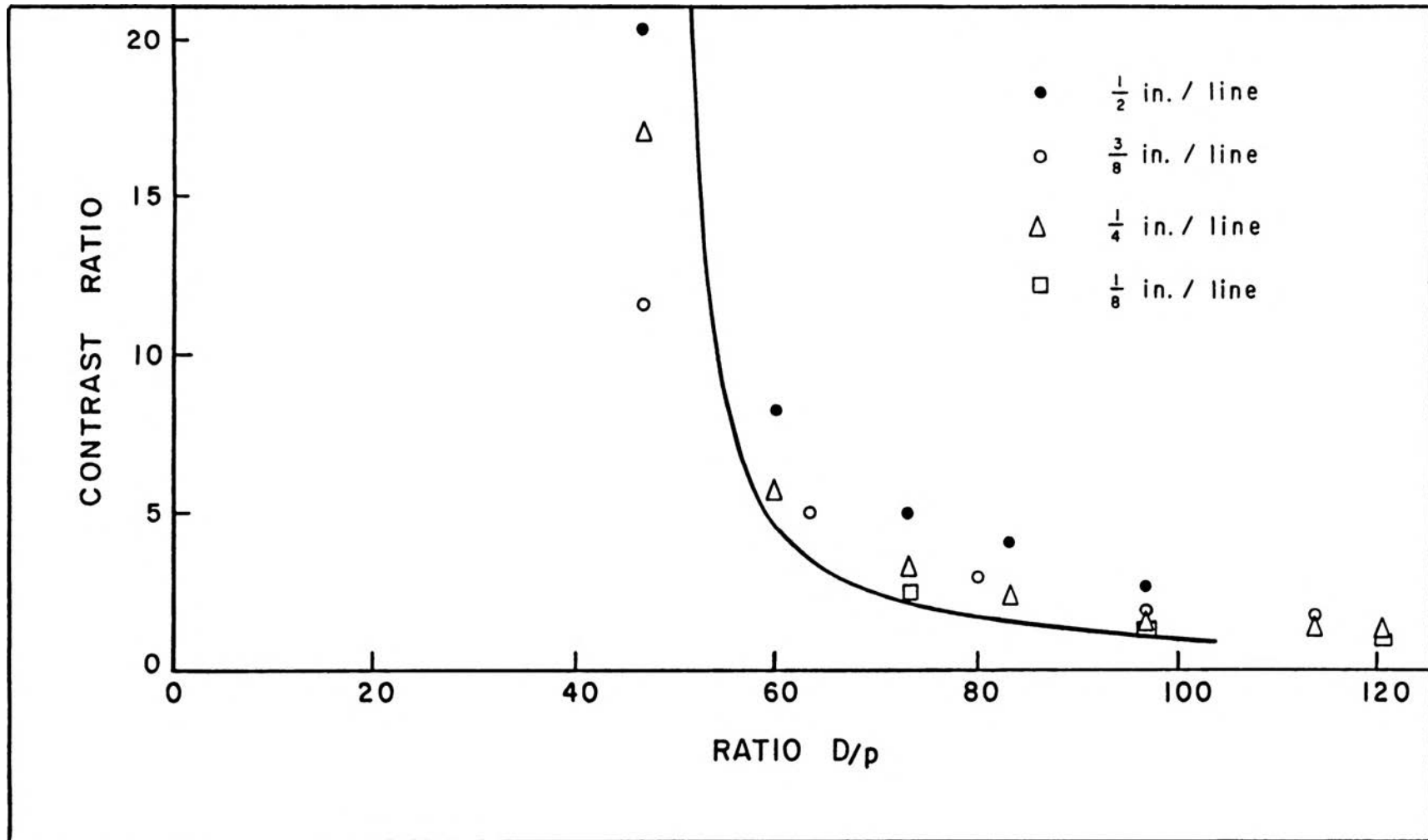
FIGURE 10. Contrast by Experiment and Theory

The scaled contrast ratio as determined experimentally is compared to the theoretical result with the effect of background illumination included.

VI. PRINCIPLE EFFECT

The principle effect in a physical situation depends on the relationships between the divergence angle, the wavelength of light, and the grating period. The behavior of the system differs for the divergence effect and the diffraction effect. When the divergence effect is dominant, the intensity obeys the convolution formula given by Equation (8), Section IV and has a linear scaling law. When the diffraction effect is dominant, the intensity obeys Equation (8) in Section III and has a squared scaling law.

The divergence angle is a measure of how rapidly the light spreads behind the grating. In terms of the mathematical description given, the size of the impulse function is proportional to the divergence angle (see Equation (3), Section IV).

The first order diffraction angle, ϕ_d, is the comparable measure for the diffraction case. This angle is defined as follows.

$$\phi_d = \lambda/p \qquad (1)$$

When this angle is small, it approximates the angular half width at which the intensity from a single slit is down by a factor of one half. This slit has a width of $\frac{1}{2}p$. The derivation is given by Crawford [17] and many other elementary physics and optics books. The percentage of energy

which falls within an angular width can be found using the following approximation [18].

$$E = 1 - \lambda R / 2\pi^2 \phi \qquad (2)$$

where E = fraction of energy within angular width

λ = wavelength

ϕ = angular half width

R = aperture perimeter-to-area ratio.

The perimeter-to-area ratio, R, for each slit of the infinite grating is 4/p. The fraction of energy within the first order diffraction angle is

$$E = 1 - \lambda R / 2\pi^2 \phi_d = 1 - \lambda(\frac{4}{p})(\frac{1}{2\pi^2})(\frac{p}{\lambda}) = 1 - \frac{2}{\pi^2} = 0.80.$$

Therefore, eighty percent of the energy from each slit is within the angular half-width ϕ_d.

The principle effect is then determined from the size of the associated angles. The divergence effect dominates if

$$\theta_d > \phi_d = \lambda/p.$$

The diffraction effect dominates if

$$\theta_d < \phi_d = \lambda/p.$$

If the angles are roughly equal, both effects will be observable.

VII. CONCLUSION

The contrast in the shadow of a grating decreases and is eventually eliminated as the distance behind the grating is increased. This phenomenon severely limits the range of the shadow moire technique which relies on the contrast of the shadow.

A cause of the contrast reduction is diffraction by the grating. The intensity pattern in the Fresnel region is given explicitly in Section III by Equation (8). In general, this pattern is very complicated. It follows a squared scaling law.

The other cause of the contrast reduction is divergence in the incident illumination. The intensity pattern due to this effect is relatively simple. It is given explicitly in Section IV by Equation (8) and is clearly shown in Figure 6. The contrast ratio takes on the closed form

$$\text{C.R.} = 1/(4\theta_d D/p - 1). \tag{1}$$

This relationship was experimentally verified. The scaling law for this effect is linear.

In a physical situation, both diffraction and divergence occur. For a single slit in the grating, the angular half-width of the diffracted light is the first order diffraction angle which is

$$\phi_d = \lambda/p. \tag{2}$$

The angular half-width for the divergence effect is the divergence angle, θ_d, which depends on the light source. The principle effect in a given situation is determined by which angle, ϕ_d or θ_d, is largest.

The shadow can be observed for distances less than the distance at which the contrast ratio is unity. When diffraction is dominant, this distance is

$$p^2/2\lambda = p/2\theta_d. \tag{3}$$

When divergence is dominant, the distance is

$$p/2\phi_d. \tag{4}$$

These results are derived for a binary grating, but give insight into the behavior for apertures of similar structure. The methods employed here can be used to determine the properties of more general apertures.

The analysis in this thesis is done for monochromatic light and produces the explicit results that have been described. For incoherent light the analysis is more complicated. The intensities calculated separately for each wavelength present must be added to obtain the total intensity. For the divergence case, the intensity distribution is unchanged because each wavelength has a similar pattern. For the diffraction case, the distributions due to each wavelength is different. Thus, the total intensity distribution is very complicated. The distance at which

the contrast ratio is unity can no longer be easily pre-
dicted.

The scaling laws derived for diffraction and diver-
gence have great value. These laws allow tests to be
conducted on conveniently sized gratings and the results to
be applied to other gratings. The only restriction is that
the same effect dominates for both sets of gratings.

The versatility and usefulness of the shadow moire
technique can be improved through an understanding of the
shadow contrast. The characteristics of the grating and
the source can be manipulated to obtain a desired range or
a desired scaling law. The fundamental limit of the range
can be calculated when diffraction dominates (and monochro-
matic light is used) and when divergence dominates.

This study does not address the situation in which the
diffraction effects and the divergence effects are compara-
ble. An application in which both effects are significant
can easily occur. A general understanding of the contrast
variation behind gratings requires further study in this
area.

The results in this thesis can be improved by applying
more general conditions. For instance, diffraction effects
due to incoherent illumination should be studied. Also,
the divergence results can be extended by using a more
accurate impulse response function (e.g. a cosinusoidal
pulse rather than a rectangular pulse).

BIBLIOGRAPHY

1. Lord Rayleigh. "On the Manufacture and Theory of Dif-
   fraction-Gratings", Scientific Papers, Vol. 1, New
   York: Dover Publications, Inc., 1964, 208-9; Philo-
   sophical Magazine, Vol. 47 (1874), 81-93 and 193-205.

2. Guild, John. The Interference Systems of Crossed
   Diffraction Gratings, Oxford: Clarendon Press, 1956,
   1-8 and 91-144.

3. Durelli, Augusto J. and Parks, V. J. Moire Analysis
   of Strain, Englewood Cliffs, New Jersey: Prentice-
   Hall, Inc., j1970.

4. Andonian, A. T. "A Simplified Moire Analysis for Two-
   Dimensional Strain Measurements", Experimental Tech-
   niques, (June, 1983), 25-7.

5. McDonach, A., McKelvie, J., MacKenzie, P., and Walker,
   C. A. "Improved Moire Interferometry and Applications
   in Fracture Mechanics, Residual Stress and Damaged
   Composites", Experimental Techniques, (June, j1983),
   20-4.

6. Baker, B.B. and Copson, E.T. The Mathematical Theory
   of Huygens' Principle, Second Ed., New York: Oxford
   University Press, 1930.

7. Lipson, S.G. and Lipson, H. Optical Physics,
   Cambridge: University Press, 1969, 136-48.

8. Born, Max, and Wolf, Emil. <u>Principles of Optics</u>, New York, London, Paris, and Los Angeles: Pergamon Press, Inc., 1959, 386-91.

9. Goodman, Joseph W. <u>Introduction to Fourier Optics</u>, San Francisco, New York, St. Louis, Toronto, London, and Sydney: McGraw-Hill Book Company, 1968, 57-61.

10. Lord Rayleigh. "On Copying Diffraction-Gratings, and on Some Phenomena Connected Therewith", <u>Scientific Papers</u>, Vol. 1, New York: Dover Publications, Inc., 1964, 504-12; <u>Philosophical Magazine</u>, Vol. 11 (1881), 196-205.

11. Montgomery, W. Duane. "Self-Imaging Objects of Infinite Aperture", <u>Journal of the Optical Society of America</u>, Vol. 57, No. 6, (June, 1967), 772-78.

12. Chavel, P. and Strand, T.C. "Range Measurement Using Talbot Diffraction Imaging of Gratings", <u>Applied Optics</u>, Vol. 23, No. 6 (March, 1984), 862-71.

13. Cowley, J.M. and Moodie, A.F. "Fourier Images: II - The Out-of-focus Patterns", <u>The Proceedings of the Physical Society</u> (London), Section B: Vol. 70 (May, 1957), 497-504.

14. Arkadiew, W. "Die Fresnelschen Beugungserscheinungen", <u>Physikalische Zeitschrift</u>, Vol. 14, (1913), 832-5.

15. Sommerfeld, Arnold. Optics, translated by Otto Laporte and Peter A. Moldauer, New York and London: Academic Press, 1964, 220-1.

16. McGillelm, Clare D. and Cooper, George R. Continuous and Discrete Signal and System Analysis, New York, Chicago, San Francisco, Atlanta, Dallas, Montreal, Toronto, London, and Sydney: Holt, Rinehart, and Winston, Inc., 1974, 68-77.

17. Crawford, Frank S., Jr. Waves, San Francisco, New York, St. Louis, Toronto, London, and Sydney: McGraw-Hill Book Company, 1968, 451-518.

18. Clark, Peter P., Howard, James W., and Freniere, Edward R. "Asymptotic Approximation to the Encircled Energy Function for Arbitrary Aperture Shapes", Applied Optics, Vol. 23, No. 2 (January, 1984), 353-7.

VITA

Steve Eugene Watkins was born on October 17, 1960 in Houston, Missouri. His parents are Eugene and Jessie Watkins. He received his primary and secondary education in Salem, Missouri. After graduating from high school, he attended the University of Missouri-Rolla. He received a Bachelor of Science degree in Electrical Engineering in July, 1983.

He has been enrolled in the Graduate School of the University of Missouri-Rolla since August 1983. From August 1983 to May 1984, he held a Chancellor's Fellowship and was a Graduate Teaching Assistant and a Graduate Research Assistant. From August 1984 to May 1985, he held a National Science Foundation Fellowship.